J|A|C|S
ARTICLES
Published on Web 10/23/2004

Synthesis of Eu^{3+}-Doped Core and Core/Shell Nanoparticles and Direct Spectroscopic Identification of Dopant Sites at the Surface and in the Interior of the Particles

Olaf Lehmann, Karsten Kömpe,[†] and Markus Haase*,[†]

Contribution from the Institut für Physikalische Chemie, Universität Hamburg, Bundesstrasse 45, D-20146 Hamburg, Germany

Received December 19, 2003; E-mail: markus.haase@uni-onsabrueck.de

Abstract: A variety of redispersible Eu^{3+}-doped $LaPO_4$ nanoparticles have been prepared in a high-boiling coordinating solvent mixture, and the Eu^{3+} lattice sites of these materials have been investigated by luminescence line-narrowing measurements. In this spectroscopic method, Eu^{3+} ions occupying different lattice sites are selectively excited with a tunable narrow-bandwidth laser system and distinguished by their luminescence spectra ("site-selective spectroscopy"). Depending on the concentration of the dopant, up to three different lattice sites could be identified in the interior of the $LaPO_4$ nanoparticles. These sites correspond to those known from bulk $LaPO_4$. In addition, a variety of surface sites is observed, which could be converted completely into bulk sites by overgrowing the nanoparticles with a shell of pure $LaPO_4$. The surface sites are identical to those obtained by reacting Eu^{3+} with the surface of pure $LaPO_4$ nanoparticles. The spectroscopic properties of Eu^{3+}-doped $LaPO_4$ nanoparticles differ from those of pure $EuPO_4$ nanoparticles, which were also investigated. Remarkably, the core/shell synthesis investigated in this paper allows one to prepare doped nanoparticles that contain no other dopant sites than those known from the corresponding bulk material.

Introduction

Lanthanide-doped nanoparticles form a class of highly luminescent materials that display narrow emission bands as well as luminescence decay times in the range of milliseconds.[1] Doped nanoparticles prepared in coordinating solvent mixtures are redispersible in common organic solvents and therefore combine high colloidal solubility with solid-state properties such as a rigid crystal environment for the dopant ions.[2] Similar to luminescent semiconductor nanoparticles or quantum dots, they are attractive for a variety of applications.[3−5]

The incorporation of dopant ions into the lattice of nanocrystals and their distribution inside these crystals have been discussed in several publications. In the case of $CdS:Er^{3+}$ it was found that the dopant ions are mainly deposited onto the surface of the nanoparticles.[6] Manganese ions have been successfully doped into the crystal lattice of CdSe nanocrystals and show an increased manganese concentration near the particle surface.[7] Strong surface enrichment of the dopant ions has been observed also in SnO_2:Sb nanoparticles and is found to depend on the antimony source employed in the synthesis.[8]

In general, functional doping of a nanomaterial requires that the dopant ions substitute metal ions of the host lattice, i.e., that they occupy lattice sites of the host metal ions. To prove the latter, a local structural probe is required that provides information about the geometry or the crystal field in the surroundings of the dopant ion.[9] One such structural probe is the Eu^{3+} ion, showing a luminescence line spectrum that is very sensitive to the symmetry and the bond distances of the lattice site. In earlier papers it was shown that Eu^{3+} doped into YVO_4 and $LaPO_4$ nanoparticles display luminescence line spectra identical to those known from the corresponding bulk materials.[10−13] This indicates that most dopant ions occupy the same lattice sites as in the bulk material, despite the small particle size of 5 nm and the comparatively low temperature at which these nanocrystals are grown. This was a surprising result, since for a 5 nm particle and a random distribution of dopant ions about 25−30% of the Eu^{3+} ions are expected to occupy lattice sites at the particle surface. Consequently, the Eu^{3+} ions in these particles are either concentrated in lattice sites in the

[†] Current address: Institut für Chemie, Universität Osnabrück, Barbarastr. 7, 49076 Osnabrück, Germany.

(1) Stouwdam, J. W.; Hebbink, G. A.; Huskens, J.; Van Veggel, F. C. J. M. *Chem. Mater.* **2003**, *15*, 24, 4604.
(2) Meyssamy, H.; Riwotzki, K.; Kornowski, A.; Naused, S.; Haase, M. *J. Phys. Chem. B* **2000**, *104*, 2824.
(3) Hebbink, G. A.; Stouwdam, J. W.; Reinhoudt, D. N.; van Veggel, F. J. M. *Adv. Mater.* **2002**, *14*, 1147.
(4) Schuetz, P.; Caruso, F. *Chem. Mater.* **2002**, *14*, 4509.
(5) Riwotzki, K.; Meyssamy, H.; Schnablegger, H.; Kornowski, A.; Haase, M. *Angew. Chem., Int. Ed.* **2001**, *40*, 573.
(6) Schmidt, T.; Müller, G.; Spanhel, L.; Kerkel, K.; Forchel, A. *Chem. Mater.* **1998**, *10*, 65.
(7) Mikulec, F. V.; Kuno, M.; Bennati, M.; Hall, D. A.; Griffin, R. G.; Bawendi, M. G. *J. Am. Chem. Soc.* **2000**, *122*, 2532.
(8) McGinley, C.; Borchert, H.; Pflughoefft, M.; Al Moussalami, S.; de Castro, A. R. B.; Haase, M.; Weller, H.; Möller, T. *Phys. Rev. B* **2001**, *64*, 245312.
(9) Tissue, B. M. *Chem. Mater.* **1998**, *10*, 2837.
(10) Riwotzki, K.; Haase, M. *J. Phys. Chem. B* **1998**, *102*, 10129.
(11) Huignard, A.; Gacoin, T.; Boilot, J.-P. *Chem. Mater.* **2000**, *12*, 1090.
(12) Huignard, A.; Buissette, V.; Laurent, G.; Gacoin, T.; Boilot, J.-P. *Chem. Mater.* **2002**, *14*, 2264.
(13) Huignard, A.; Buissette, V.; Franville, A.-C.; Gacoin, T.; Boilot, J.-P. *J. Phys. Chem. B* **2003**, *107*, 6754.

center of the nanoparticles or the emission of Eu^{3+} in surface sites is partly quenched and obscured by some inhomogeneous broadening of the luminescence lines. In fact, very recently it was shown that additional Eu^{3+} sites exist in our nanomaterials.[14] In the paper presented here we have used the luminescence line-narrowing technique to selectively excite Eu^{3+} ions in our europium-doped nanocrystals with a tunable narrow-bandwidth laser system. The method allows one to distinguish Eu^{3+} ions in different lattice sites by their luminescence spectra. The Eu^{3+} ion has frequently been used as a structural probe for a variety of materials, including nanocrystalline Y_2O_3:Eu^{3+} prepared by a laser ablation technique,[15] because its luminescence spectrum consists of sharp emission lines and the splitting and the intensity of these lines depend on the crystal field at the lattice site. Since the spectrum is only affected by the first two or three coordination shells around the Eu^{3+} ion, however, it can be difficult or even impossible to determine *where* inside the sample this Eu^{3+} site is located. To overcome this deficiency of the method, we make use of a recently developed synthesis technique that allows one to epitaxially grow a shell of undoped $LaPO_4$ around the doped $LaPO_4$ nanoparticles. By analyzing how the luminescence spectra are affected by the presence of the shell, we are able to assign each spectrum to Eu^{3+} sites in the interior or at the surface of the nanoparticles.

All nanocrystals employed in this paper are fully redispersible in organic solvents to give clear and transparent colloidal solutions. The following abbreviations are used throughout the text:

$LaPO_4$:Eu^{3+} (5%) and $LaPO_4$:Eu^{3+} (1%) core particles refer to lanthanum phosphate nanoparticles doped with 5% and 1% europium, respectively. Overgrowing these particles with a shell of pure $LaPO_4$ leads to the respective core/shell nanoparticles, in the following referred to as $LaPO_4$:Eu^{3+} (5%)/$LaPO_4$ and $LaPO_4$:Eu^{3+} (1%)/$LaPO_4$. In a similar way, $LaPO_4$/surface Eu^{3+} nanoparticles were prepared by reacting a colloidal solution of pure $LaPO_4$ nanoparticles with Eu^{3+} in the presence of excess phosphate. Finally, nanoparticles of pure $EuPO_4$ have been prepared with two different mean particle sizes. These systems are distinguished in the text by the terms "large" and "small".

Results and Discussion

The nanoparticles were prepared with an excess of phosphoric acid in a coordinating solvent mixture as described previously.[16] In all cases, the yields obtained after synthesis indicated complete conversion of the metal ions into metal phosphate nanoparticles. In Figure 1 the X-ray powder diffraction data of all nanomaterials are summarized. For all systems except for the small $EuPO_4$ nanoparticles (Figure 1c), the XRD patterns are very similar to those recently published for $CePO_4$:Tb^{3+} nanoparticles and $CePO_4$:Tb^{3+}/$LaPO_4$ core/shell particles.[17] The peak positions and intensities are in accord with literature values for the corresponding $EuPO_4$ and $LaPO_4$ bulk materials, both crystallizing in the monoclinic monazite phase (Figure 1a,d, compare also with ref 16).

A very small shift of the diffraction lines is expected for the doped materials, because the ionic radius of the Eu^{3+} ions is about 7% smaller than the ionic radius of the La^{3+} ions. However, this shift cannot be measured in our nanocrystalline samples, because the europium concentration is rather low and the width of the diffraction lines is strongly broadened due to the small size of the crystallites. The narrowest diffraction peaks are observed for the core/shell particles, i.e., $LaPO_4$:Eu^{3+} (1%)/$LaPO_4$ (Figure 1h) and $LaPO_4$:Eu^{3+} (5%)/$LaPO_4$ (Figure 1i), where a shell of a material with virtually identical lattice constants enlarges the size of the core particle. The particle sizes can be estimated by using the Debye−Scherrer formula, which yields a mean particle diameter of approximately 8 nm for the large $EuPO_4$ particles (Figure 1b) and of approximately 6 nm for the $LaPO_4$:Eu^{3+} (Figure 1f,g) and the $LaPO_4$/surface Eu^{3+} particles (Figure 1e). As was the case for the $CePO_4$:Tb^{3+}/$LaPO_4$ core/shell particles, a slight anisotropy of the peak widths is also observed for the $LaPO_4$ core/shell systems. In particular, the (200) peak is narrower than the (012) and (120) peaks, indicating a slight elongation of the particles in the (100) direction. Analysis of the peak widths yield particle dimensions of 14 nm in length and approximately 8 nm in width for the core/shell particles (Figure 1h,i). Further results of the peak width analysis are included in Figure 1.

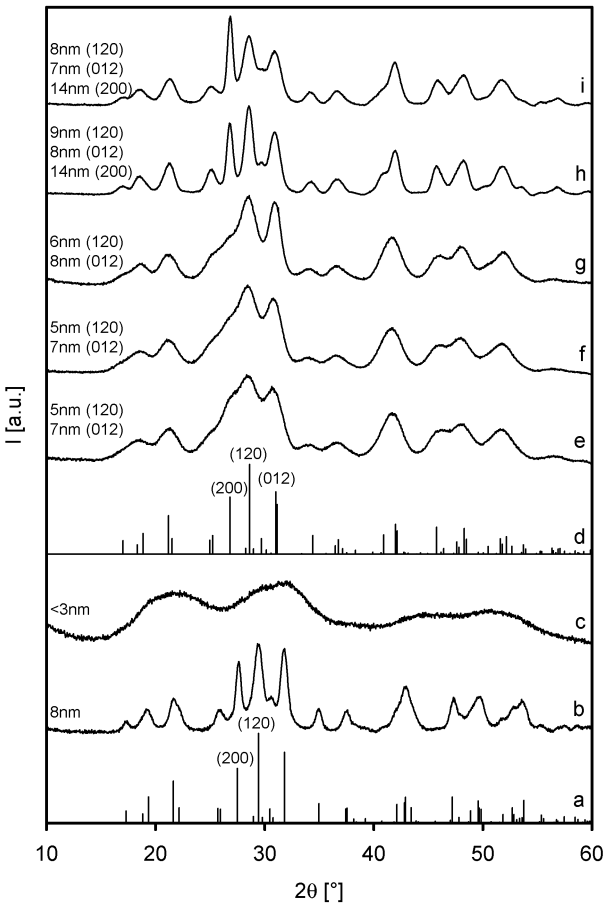

Figure 1. X-ray diffraction patterns of the nanoparticles with the corresponding particle diameters (given on the left): (a) line positions of the monazite $EuPO_4$ lattice [PDF 83−0656], (b) large $EuPO_4$, (c) small $EuPO_4$, (d) line positions of the monazite $LaPO_4$ lattice [PDF 84-0600], (e) $LaPO_4$/surface Eu^{3+}, (f) $LaPO_4$:Eu^{3+} (1%), (g) $LaPO_4$:Eu^{3+} (5%), (h) $LaPO_4$:Eu^{3+} (1%)/$LaPO_4$, and (i) $LaPO_4$:Eu^{3+} (5%)/$LaPO_4$.

Figure 2 displays overview and high-resolution TEM images (insets) of the $LaPO_4$:Eu^{3+} (1%) nanoparticles (a), $LaPO_4$:Eu^{3+} (1%)/$LaPO_4$ core/shell particles (b), $LaPO_4$/surface Eu^{3+} par-

(14) Wang, R. Y.; Lifshitz, E. *J. Lumin.* In press.
(15) Williams,D. K.; Yuan, H.; Tissue, B. M. *J. Lumin.* **1999**, *83*−*84*, 297.
(16) Lehmann, O.; Meyssamy, H.; Kömpe, K.; Schnablegger, H.; Haase, M. *J. Phys. Chem. B* **2003**, *107*, 7449.
(17) Kömpe, K.; Borchert, H.; Storz, J.; Lobo, A.; Adam, S.; Möller, T.; Haase, M. *Angew. Chem., Int. Ed.* **2003**, *42*, 5513.
(18) van de Hulst, H. C. *Light Scattering by Small Particles;* Dover Publications: Mineola, NY, 1981 (ISBN 0486642283).

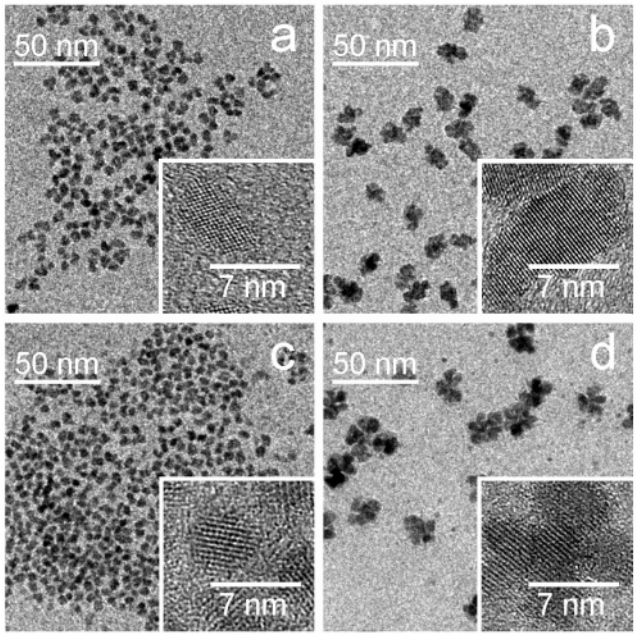

Figure 2. Transmission electron microscope (TEM) images of (a) $LaPO_4$:Eu^{3+} (1%) particles, (b) $LaPO_4$:Eu^{3+} (1%)/$LaPO_4$ core/shell particles, (c) $LaPO_4$/surface Eu^{3+} particles, and (d) large $EuPO_4$ particles. Insets: high-resolution images.

ticles (c), and the large $EuPO_4$ nanoparticles (d). The $LaPO_4$:Eu^{3+} nanoparticles (a) and the $LaPO_4$/surface Eu^{3+} nanocrystals (c) exhibit narrow particle size distributions and a mean particle diameter of about 6 nm. This value is in accord with the XRD data given above and shows that deposition of the Eu^{3+} ions (i.e., 5 mol % with respect to the lanthanum content) onto the surface of the $LaPO_4$/surface Eu^{3+} nanocrystals did not significantly increase the particle diameter of the $LaPO_4$ core. In contrast, the size of the $LaPO_4$:Eu^{3+}/$LaPO_4$ core/shell particles (b) is significantly enlarged with respect to the diameter of the $LaPO_4$:Eu^{3+} nanoparticles (a), since a large amount of La^{3+} and phosphate is used to grow the shell (compare with the Experimental Section). The core/shell particles are not very uniform in shape and most of them are elongated, having an approximate length of 14 nm and a width of 8 nm. The large $EuPO_4$ nanoparticles shown in Figure 2d were obtained by heating of the reaction mixture for 16 h. Under these conditions, the small particles start to grow, but in contrast to $LaPO_4$ nanoparticles, this growth is accompanied by agglomeration and partial fusion of the nanocrystalline domains as described earlier.[16] This is clearly seen in the figure. Since we did not extend heating for too long, the resulting agglomerates remained separated and did not precipitate. In contrast to the small $EuPO_4$ particles, the larger particles clearly display the same monazite phase as bulk $EuPO_4$ (Figure 1a).

Since the small $EuPO_4$ nanoparticles are too tiny to either obtain high-quality TEM images or an analyzable XRD pattern (Figure 1b), their particle size was determined by dynamic light scattering measurements.[18] The latter indicated a hydrodynamic diameter of 3.4 nm in colloidal solution. For $GdPO_4$ nanoparticles, which are synthesized by the same procedure and display the same XRD pattern, a diameter of 2.6 nm was measured by small-angle X-ray scattering.[16] Since the latter technique ignores the contribution of the ligand shell to the particle size, this value is in accord with the larger value measured by dynamic light scattering.

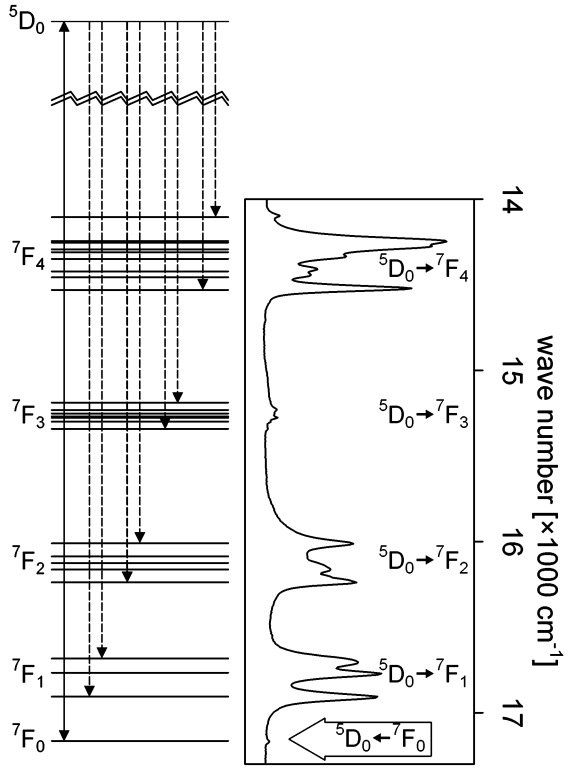

Figure 3. (Left) Part of the energy level scheme of an Eu^{3+} ion. Each ^7F_J state ($J = 0, 1, 2, 3, 4$) is split in up to $2J + 1$ sublevels by the crystal field. Excitation to the $^5D_0$ state results in luminescence emission due to relaxation to all of these sublevels (as indicated by broken arrows for some of these transitions). In site-selective spectroscopy experiments, the Eu^{3+} ions are excited via their $^5D_0 - {}^7F_0$ transition (solid arrow). (Right) The Eu^{3+} luminescence spectrum of $LaPO_4$:Eu^{3+} nanocrystals measured at room temperature. The spectrum is rotated by 90° and corresponds to the total emission of all Eu^{3+} sites.

The spectroscopic properties of the Eu^{3+} ion are determined by transitions between its f-electron energy levels. Part of the f-electron level scheme of the Eu^{3+} ion is given in Figure 3, where the common $^{2S+1}L_J$ notation is used for the levels, S, L, and J referring to spin, orbital, and total angular momentum, respectively. The figure only displays the $^5D_0$ level and the ^7F_J levels, with $J = 0, 1, 2, 3$, and 4. Each of these levels can be split in up to a maximum of $2J + 1$ sublevels by the crystal field, as indicated in the figure. Luminescence transitions are observed between the $^5D_0$ level and each of these sublevels. For clarity, only a limited number of these transitions are given as broken arrows in Figure 3. The right-hand side of the figure shows the Eu^{3+} luminescence spectrum of $LaPO_4$:Eu^{3+} nanocrystals at room temperature. The spectrum has been rotated by 90° in order to display more clearly the connection between the f-electron energy levels and the luminescence lines of the spectrum. Since the spectrum has been recorded under excitation with UV light, i.e., under conditions where all Eu^{3+} ions are excited simultaneously, it corresponds to the total emission of all Eu^{3+} ions of the sample.

In the following paragraphs, a large number of luminescence spectra will be shown, where the Eu^{3+} ions are excited via their $^7F_0 - {}^5D_0$ transition, given as a solid arrow in the energy level scheme of Figure 3. This $^7F_0 - {}^5D_0$ transition always consists of a single line, because neither the $^7F_0$ state nor the $^5D_0$ state can be split into sublevels by the crystal field. The energy of this transition, however, depends on the crystal field of the Eu^{3+}

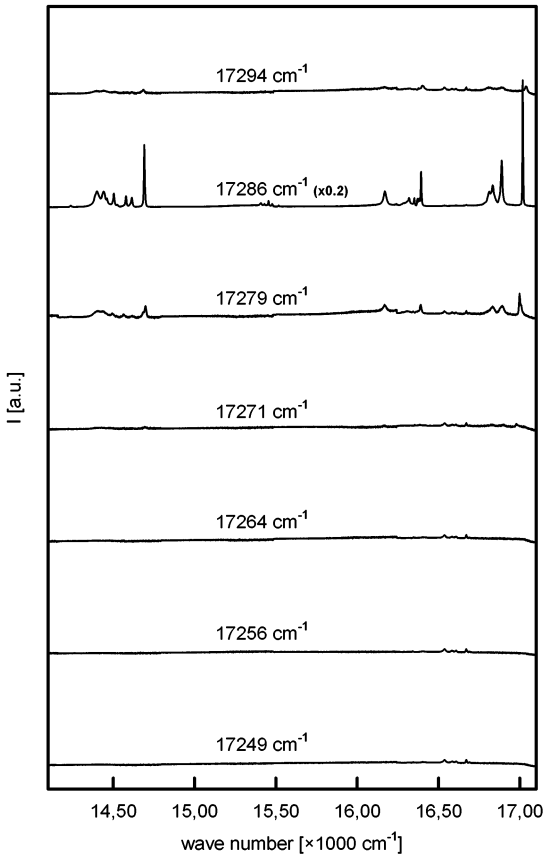

Figure 4. Site-selective fluorescence spectra of $LaPO_4:Eu^{3+}$ (1%)/$LaPO_4$ core/shell particles, excited at 30 K at the wavenumbers indicated. The spectrum of the majority europium site is identical to the emission of the europium M-site in bulk $LaPO_4:Eu^{3+}$. Its intensity in the figure is reduced by a factor of 5. The weak emission under 17 279 cm^{-1} excitation corresponds to the europium L-site of the bulk material.

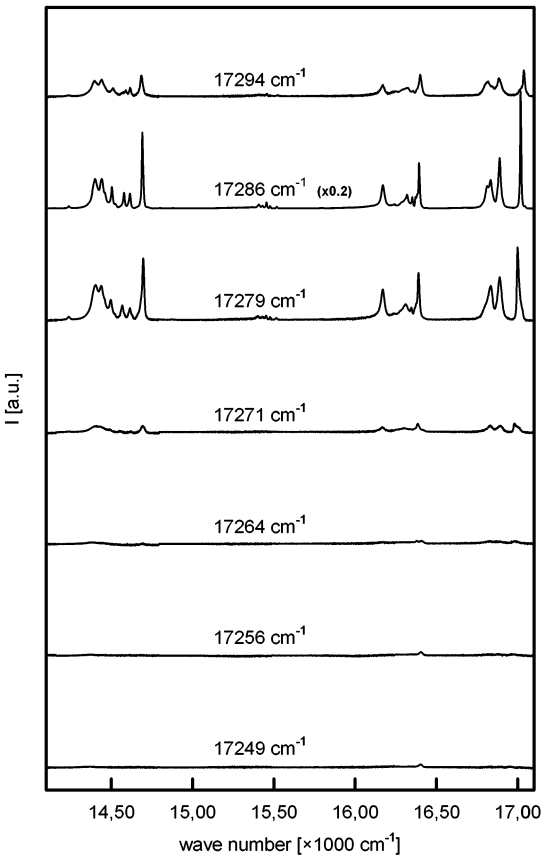

Figure 5. Site-selective fluorescence spectra of $LaPO_4:Eu^{3+}$ (5%)/$LaPO_4$ core/shell particles, excited at 30 K at the wavenumbers indicated. The Eu^{3+} spectra correspond to the L-site (17 279 cm^{-1} excitation), M-site (17 286 cm^{-1} excitation), and H-site (17 294 cm^{-1} excitation) of bulk $LaPO_4:Eu^{3+}$. Due to energy transfer processes, the spectra of the L- and H-sites contain a weak contribution of the M-site spectrum.

lattice site, resulting in inhomogeneous broadening of this transition if the sample contains Eu^{3+} ions in different lattice sites. The observed line width of the $^7F_0-^5D_0$ transition in our samples is at least 50 cm^{-1} (from approximately 17 250 cm^{-1} to approximately 17 300 cm^{-1}), which in fact indicates the presence of a variety of Eu^{3+} lattice sites in the nanocrystals.

In the work presented here, the different Eu^{3+} lattice sites have been selectively excited by using a tunable laser source with a very narrow laser line width of <0.1 cm^{-1}, and the luminescence spectrum of each site has been recorded separately ("site-selective spectroscopy"). The following figures show the luminescence spectra of dried nanoparticle powders under site-selective excitation at 30 K (Figures 4−9). Each sample has been selectively excited at seven different laser wavelengths (excitation energies), all of which were located in the spectral region of the inhomogeneously broadened $^7F_0-^5D_0$ transition. The resulting seven luminescence spectra are shown in each figure along with the excitation energies given in wavenumbers above each spectrum. The luminescence spectra of all sites consist of luminescence lines that form well-separated groups as in the spectrum given in Figure 3. The lines of each group correspond to transitions from the $^5D_0$ state to the sublevels of a ^7F_J state. For $J = 1, 2, 3, 4$, these transitions lie in the visible region; i.e., the $^5D_0 \rightarrow {}^7F_4$ transitions are always in the range from 14 220 to 14 720 cm^{-1}, the $^5D_0 \rightarrow {}^7F_3$ transitions are observed always from 15 390 to 15 520 cm^{-1}, the $^5D_0 \rightarrow {}^7F_2$ transitions from 16 120 to 16 430 cm^{-1}, and the $^5D_0 \rightarrow {}^7F_1$ transitions from 16 760 to 17 050 cm^{-1}. However, the intensity and the splitting of the luminescence lines of each group are different for the different lattice sites. This is because the crystal field at each lattice site determines the splitting of the ^7F_J states as well as the probabilities for transitions from the $^5D_0$ state to the resulting sublevels.

Site-selective excitation of the $LaPO_4:Eu^{3+}$ (1%)/$LaPO_4$ core/shell nanoparticles reveals only one major Eu^{3+} site in this material (Figure 4). The luminescence spectrum of a second, weaker site is observed under excitation at 17 279 cm^{-1}. Note that we have reduced the luminescence intensity of the majority site (excited at 17 286 cm^{-1}) by a factor of 5 in the figure. Comparison of these spectra with the luminescence spectra given by Dexpert-Ghys et al.[19] for bulk $LaPO_4:Eu^{3+}$ shows that both sites are also observed in the bulk material. The majority site excited at 17 286 cm^{-1} is known as the M-site and displays additional vibronic lines as discussed in the literature.[19] Further comparison with ref 19 shows the weaker intensity site to be the L-site of the bulk material.

We do not compare here the width of the emission lines of the M-site between the bulk and the nanocrystalline material, since the width observed for our nanocrystals is already strongly affected by the limited spectral resolution of our monochromator. We would expect a broader line width for the nanocrystals, for instance, because in nanocrystalline materials the reconstruction

(19) Dexpert-Ghys, J.; Mauricot, R.; Faucher, M. D. *J. Lumin.* **1996**, *69*, 203.

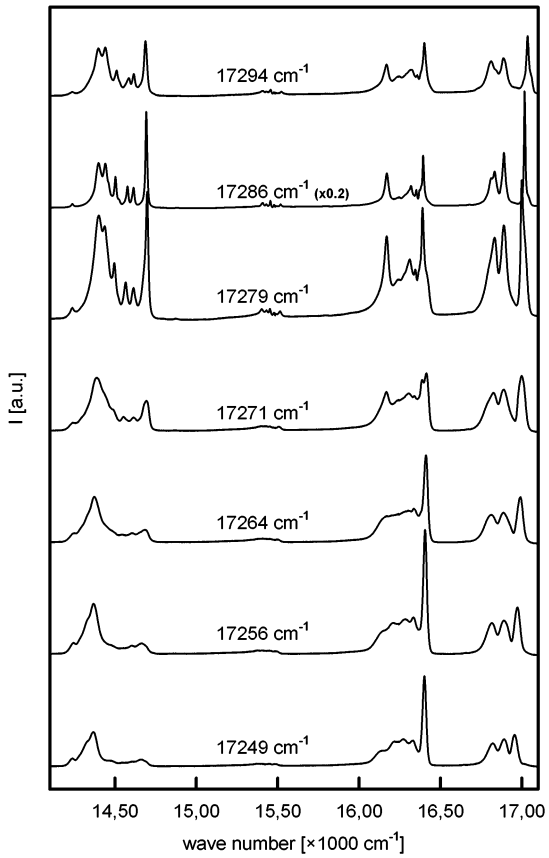

Figure 6. Site-selective fluorescence spectra of $LaPO_4:Eu^{3+}$ (5%) nanoparticles without shell, excited at 30 K at the wavenumbers indicated. Without the $LaPO_4$ shell, the $LaPO_4:Eu^{3+}$ (5%) nanoparticles display spectra of additional Eu^{3+} sites over the entire excitation range.

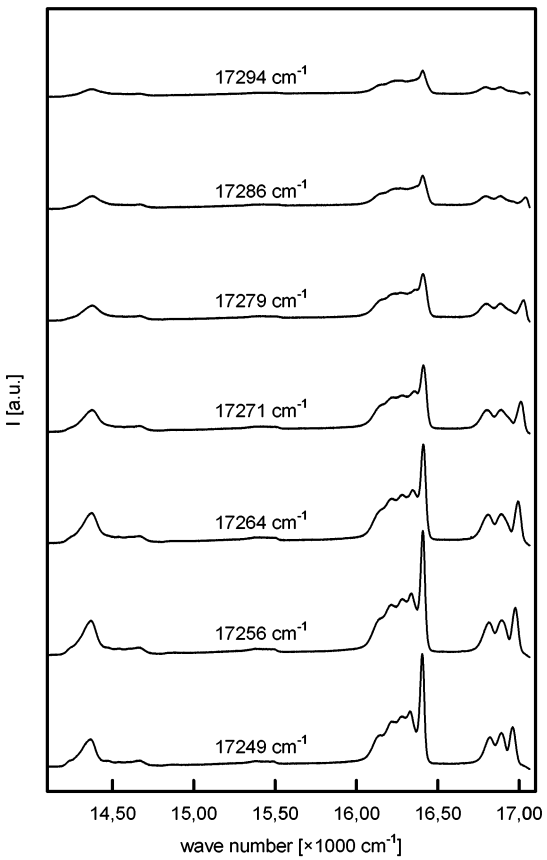

Figure 7. Site-selective fluorescence spectra of the $LaPO_4$/surface Eu^{3+} nanoparticles, excited at 30 K at the wavenumbers indicated. Only the additional Eu^{3+} sites of Figure 6 are observed.

of surface atoms can alter the bond length of atoms close to the surface, leading to a higher degree of disorder compared to the lattice of bulk materials.

Figure 5 displays the site-selective luminescence spectra of the core/shell particles with 5% europium, i.e., the $LaPO_4:Eu^{3+}$ (5%)/$LaPO_4$ nanoparticles. Again, the luminescence spectra correspond to those known from the bulk material, and the M-site, excited at 17 286 cm^{-1}, is the one with the greatest intensity by far. Two additional spectra are observed upon excitation at 17 279 and 17 294 cm^{-1}, which correspond to the L-site and the H-site of bulk $LaPO_4:Eu^{3+}$, respectively. As in the previous figure, the intensity of the M-site is reduced by a factor of 5, so the minority sites can be seen more clearly. Compared to the core/shell nanoparticles with 1% europium (Figure 4), the relative intensities of the L-site and the H-site are significantly increased. This indicates that the L- and the H-site are related to Eu^{3+} ions that have at least one other europium ion in their nearest neighborhood. Lowering the total amount of europium in the sample makes these sites less probable and only the M-site is observed. Since the M-site is the only site observed at very low Eu^{3+} concentrations, it is reasonable to assume that this site corresponds to isolated Eu^{3+} ions in the lanthanum phosphate lattice.

The three different sites in our core/shell particles doped with 5% europium are somewhat less well resolved than described in the literature for the bulk material doped with 2% europium, because the higher europium content of our sample increases the probability of energy transfer between different sites.[19] Due to the latter, the spectra of the L- and the H-site contain a weak contribution of the spectrum of the M-site.

The series of luminescence spectra is dramatically different for europium-doped nanoparticles without a $LaPO_4$ shell. Figure 6 shows the spectra of the $LaPO_4:Eu^{3+}$ (5%) core nanoparticles before a $LaPO_4$ shell was grown around them. In addition to the M-, L-, and H-sites, a new emission with comparatively broad lines appears over the whole excitation range and has its highest emission intensity under excitation at 17 256 cm^{-1}. The same additional emission is observed for the $LaPO_4$ core particles with 1% Eu^{3+} (see Figure s1 of the Supporting Information). The fact that this additional emission disappears when a shell is grown onto the particle surface already indicates that it is related to europium ions in surface sites. To further investigate the latter, we prepared $LaPO_4$ nanoparticles with europium ions only on their surface. This was achieved by reacting europium and phosphate ions with the surface of pure $LaPO_4$ particles in a manner similar to the procedure employed for the growth of $LaPO_4$ shells (see Experimental Section). An amount of 5% of europium relative to the lanthanum content of the core particle was used. Site-selective luminescence spectra of this material are shown in Figure 7. Comparison with Figure 6 shows clearly that the emission spectra are identical to the additional emission of the $LaPO_4:Eu^{3+}$ nanoparticles without a $LaPO_4$ shell. Figure 7 also proves that the emission of the surface sites overlaps with the emission of the M-, L-, and H-sites.

Under site-selective excitation at 30 K, europium ions in M-sites display luminescence decay curves with luminescence lifetimes (1/e) of 3.7, 4.0, and 4.2 ms for $LaPO_4:Eu^{3+}$ (5%)

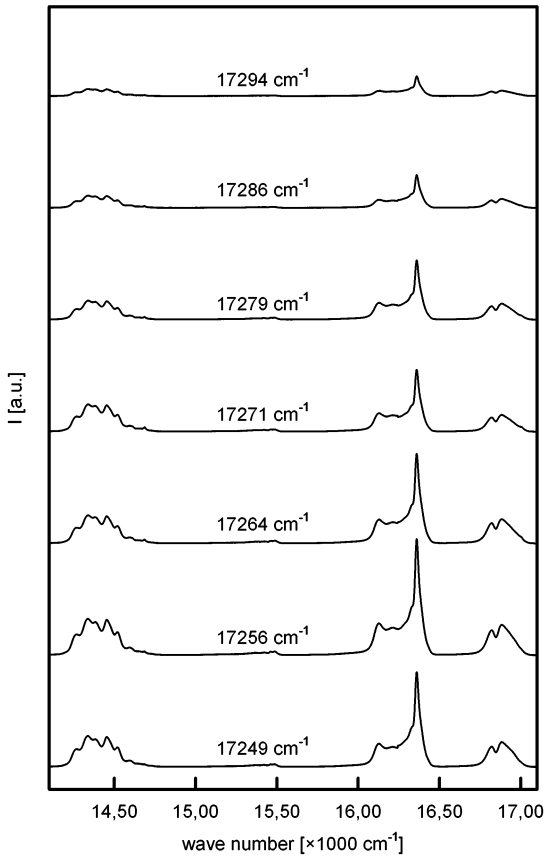

Figure 8. Site-selective fluorescence spectra of the small $EuPO_4$ nanoparticles at 30 K, excited at the indicated wavenumbers. The spectra are similar but not identical to those of Figure 7.

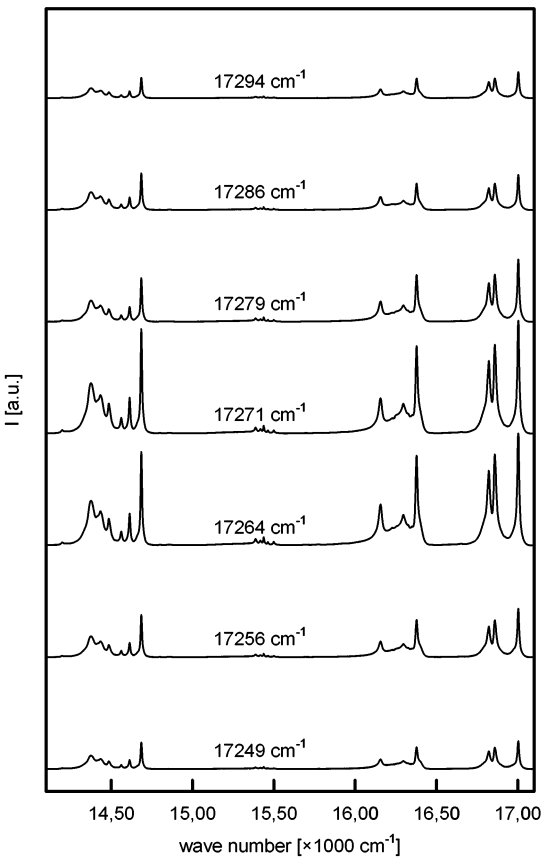

Figure 9. Site-selective fluorescence spectra of the large $EuPO_4$ nanoparticles at 30 K, excited at the indicated wavenumbers.

nanoparticles, $LaPO_4$:Eu^{3+} (1%) nanoparticles, and the two core/shell systems, respectively (see Figure s2 of the Supporting Information). The decay curves of the core and core/shell nanoparticles deviate weakly from purely monoexponential behavior, presumably due to weak energy transfer processes between the M-, L-, and H-sites as discussed in the literature for bulk $LaPO_4$:Eu^{3+} (2%).[19] In contrast, the europium surface sites of $LaPO_4$:Eu^{3+} (5%) nanoparticles, of $LaPO_4$:Eu^{3+} (1%) nanoparticles, and of $LaPO_4$/surface Eu^{3+} particles show multiexponential decay curves with mean lifetimes between 1.6 and 2.3 ms. The shorter lifetime is expected, because the proximity to high-energy vibrations of organic ligands is known to quench the luminescence of Eu^{3+} atoms. Remarkably, the mean luminescence lifetime of Eu^{3+} ions in $LaPO_4$ surface sites is still in the range of milliseconds, at least at the low temperature of 30 K.

One could still argue that the new sites are not in fact surface sites but belong to $EuPO_4$ particles that nucleated in solution separately from the doped $LaPO_4$ particles. Therefore, we additionally prepared $EuPO_4$ nanoparticles and compared their spectroscopic properties with those of doped $LaPO_4$ nanocrystals. Figure 8 shows the luminescence spectra of small $EuPO_4$ particles. In $EuPO_4$, the transport of excitation energy between Eu^{3+} ions is very effective, because the distance between adjacent Eu^{3+} ions is short due to the high concentration of europium. This energy migration over the europium sites takes place even at 30 K and results in a complete loss of site selectivity. As a consequence, all luminescence spectra of Figure 8 are very similar, despite site-selective excitation of the Eu^{3+} ions.

At first sight, the spectra of the small $EuPO_4$ particles (Figure 8) resemble those of the $LaPO_4$/surface Eu^{3+} particles (Figure 7). In fact, similarities between the spectra in Figures 7 and 8 are to be expected, because 3 nm diameter $EuPO_4$ particles contain a large number of surface atoms due to their large surface-to-bulk ratio. Consequently, Eu^{3+} surface sites contribute strongly to the luminescence spectra of the small $EuPO_4$ nanoparticles in Figure 8. However, a closer inspection of both figures shows that the details of the spectra are quite different. The most prominent differences are the position of the main peak, which is shifted from 16 410 to 16 360 cm^{-1}; the structure of the $^5D_0 \rightarrow {}^7F_1$ multiplet, which shows two resolved peaks rather than three; and the $^5D_0 \rightarrow {}^7F_4$ multiplet, which is well structured in one case but is featureless in the other. Thus, the slightly different lattice parameters of $EuPO_4$ and $LaPO_4$, the contribution of bulk sites in the case of $EuPO_4$, and probably also differences in the ligand shells of both materials lead to different crystal fields at the Eu^{3+} surface sites, which allows us to distinguish the two materials by site-selective luminescence measurements.

In a similar way, small $EuPO_4$ particles can be distinguished spectroscopically from large $EuPO_4$ nanocrystals (Figure 9). As in the case of the small $EuPO_4$ particles, energy transfer via adjacent Eu^{3+} is very effective in the large particles, and the luminescence spectra obtained under site-selective excitation are all identical. Due to the smaller surface-to-volume ratio of the large particles, however, Eu^{3+} ions in the interior of the particles contribute much more to the luminescence spectra than in the case of the small $EuPO_4$ particles. As a consequence, the luminescence spectra of Figure 9 are already very similar to

the spectrum published for bulk $EuPO_4$,[19] but they show a much stronger inhomogeneous broadening of the luminescence lines due to the strong contribution of surface sites to the spectrum. Since energy transfer between the Eu^{3+} sites leads to simultaneous emission from all sites, the luminescence decay curves of all $EuPO_4$ nanoparticles exhibit multiexponential behavior. The mean luminescence lifetimes are about 1.6 ms for the small particles and about 2.5 ms for the large $EuPO_4$ particles.

Comparison of Figures 6 and 7 with Figures 8 and 9 reveals that the site-selective luminescence spectra of the small and the large $EuPO_4$ particles are significantly different from those of the $LaPO_4$/surface Eu^{3+} and $LaPO_4$:Eu^{3+} particles. We therefore conclude that the additional Eu^{3+} sites in our $LaPO_4$:Eu^{3+} core particles are surface sites of this material and not Eu^{3+} sites of $EuPO_4$ particles additionally present in the sample.

The question remains why the luminescence lines of the surface Eu^{3+} sites are so much broader than the lines of the M-site. One likely explanation is that solvent molecules and the organic ligands coordinate to europium ions at the surface of the nanoparticles. If the number and the conformation of these molecules are not identical for all surface europium ions, different crystal fields will be the result. If a larger fraction of these surface europium ions are not isolated from another, energy transfer between adjacent surface Eu^{3+} ions will lead to inhomogeneous broadening, as in all concentrated Eu^{3+} materials. Moreover, small islands or clusters of $EuPO_4$ may exist on the surface of the $LaPO_4$:Eu^{3+} nanoparticles with similar but not identical spectroscopic properties as individual small $EuPO_4$ nanoparticles. In this case, however, one further has to assume that the clusters dissolve when a shell of $LaPO_4$ is formed around the nanoparticles. This is because our $LaPO_4$:Eu^{3+} (1%) nanoparticles display mainly the M-site after formation of the shell, i.e., the site where the europium ions have no europium neighbors.

Finally, we mention that most of our Eu^{3+}-doped $LaPO_4$ nanocrystals contain trace amounts of divalent europium (Eu^{2+}), because the nanoparticles are synthesized under reducing conditions and because the La^{3+} ion and the Eu^{2+} ion have a similar size. Moreover, protons are available in the reaction mixture for charge compensation. In contrast to the Eu^{3+} f−f-transitions discussed in this paper, the optically allowed 4f−5d-transition of the Eu^{2+} ion consists of a broad absorption band with high absorption cross section and a broad Stokes-shifted emission with short luminescence decay time. Trace amounts of Eu^{2+} ions are therefore easily excited between about 340 and 400 nm, resulting in a broad and featureless emission band between about 400 and 550 nm.

In conclusion, we have confirmed our earlier result that the crystal lattice of $LaPO_4$ nanoparticles can be successfully doped with Eu^{3+} ions in a low-temperature synthesis. The dopant ions occupy sites in the interior and at the surface of the nanoparticles, as is shown by site-selective spectroscopy. It is found that Eu^{3+} ions in the interior of the nanoparticles occupy the same lattice sites as in the bulk material and that the spectroscopic properties of Eu^{3+} ions in surface sites differ significantly from those in the interior of the particles. Since the emission lines of the former are broader and of lower intensity, the steady-state luminescence spectrum of $LaPO_4$:Eu^{3+} nanoparticles is dominated by the emission of sites in the interior of the nanoparticles and, hence, resembles the spectrum of the bulk material.

Doped nanocrystals free of surface Eu^{3+} sites have been obtained by growing a shell of $LaPO_4$ around the $LaPO_4$:Eu^{3+} nanoparticles. It is quite remarkable that these nanoparticles contain virtually no other dopant sites than those known from the corresponding bulk material, despite their small size, below 15 nm.

Experimental Section

Europium-doped $LaPO_4$ and the $EuPO_4$ nanoparticles were synthesized in high-boiling coordinating solvents according to a modified literature procedure.[16] To a clear solution of the lanthanide chloride hexahydrates [10 mmol lanthanide chlorides in total, e.g. 9.9 mmol of $LaCl_3$ with 0.1 mmol of $EuCl_3$ for the $LaPO_4$:Eu^{3+} (1%) nanoparticles] in approximately 10 mL of methanol p.a. were added 40 mmol of tributyl phosphate, and the methanol was subsequently removed with a rotary evaporator (in the case of the large $EuPO_4$ nanoparticles, only 20 mmol of tributyl phosphate was used). Diphenyl ether (30 mL) was added and the water was distilled off under reduced pressure by slowly increasing the temperature from 20 to 100 °C. Then 30 mmol of trihexylamine and 7.0 mL of a dry 2 M solution of phosphoric acid in dihexyl ether were added, and the mixture was heated to 200 °C under dry nitrogen. After 16 h the heating was stopped and the solution was allowed to cool. Subsequently, three-quarters of the reaction mixture (all of it in the case of the $EuPO_4$ nanoparticles) was removed from the reaction vessel and treated as given below to isolate the $LaPO_4$:Eu^{3+} nanoparticles as dry powders (respectively the $EuPO_4$ nanoparticles). The remaining one-quarter of the reaction mixture was used for the preparation of core/shell nanoparticles, as follows.

Separately from the reaction mixture, 15 mmol of tributyl phosphate was added to a clear solution of lanthanum chloride hexahydrate (7.5 mmol) in approximately 10 mL of methanol p.a., and the methanol was removed with a rotary evaporator. Diphenyl ether (23 mL) was added and the water removed as described above. The solution was mixed with 22.5 mmol of trihexylamine and filled into a dropping funnel connected to the reaction vessel. Next, 5 mL of the 2 M phosphoric acid solution in dihexyl ether was added to the reaction mixture, which was then heated again to 200 °C under dry nitrogen. The solution in the dropping funnel was added drop by drop over a period of 2 h to the reaction mixture kept at 200 °C. After 16 h the heating was stopped and the solution was allowed to cool.

$LaPO_4$/surface Eu^{3+} nanoparticles were prepared by first synthesizing $LaPO_4$ in an analogous way as the $LaPO_4$:Eu^{3+} particles. Then, a solution of 0.5 mmol of $EuCl_3 \cdot 6H_2O$ in 1.5 mL of diphenyl ether, 2 mmol of tributyl phosphate, and 1.5 mmol of trihexylamine was prepared and the water removed as given above. This solution was loaded into the dropping funnel and added drop by drop over 45 min to the reaction mixture of $LaPO_4$ particles, which was kept at 200 °C under nitrogen. After the addition, the reaction mixture was heated for 16 h at 200 °C and then allowed to cool to room temperature.

Subsequently, each reaction mixture was diluted with about 250 mL of methanol and was filled into a stirring (diafiltration) cell (Berghof) equipped with a 10 000 or 30 000 Da filter (Millipore). In the case of the $EuPO_4$ nanoparticles, a 5000 Da filter was used on account of their small particle size, approximately 3 nm. Using a nitrogen pressure of 3.5 bar, the solution was passed through the filter until the volume of the solution was reduced to approximately 30 mL. Thereafter, the remaining solution was again diluted with about 250 mL of methanol and the purification procedure was repeated four times. Finally, the nanoparticles were isolated from the purified colloidal solution by removing the methanol with a rotary evaporator. White powders of nanoparticles were obtained in gram amounts.

X-ray diffraction patterns of powder samples were recorded with a Philips X'pert system.

High-resolution electron micrographs of the particles were taken using a Philips CM 300 UT transmission electron microscope (TEM)

operating at an acceleration voltage of 300 kV. The microscope was equipped with a CCD camera (Gatan, model no. 694).

For the measurement of the site-selective fluorescence spectra, the nanoparticle powders were cooled to 30 K inside a closed cycle refrigerator cryostat (Leybold) and were excited with a Continuum Sunlite EX OPO pumped by a Continuum Precision II Nd:YAG laser. The fluorescence light was dispersed with a TRIAX 320 monochromator (Jobin Yvon; 1800 groove grating) and detected with a nitrogen-cooled CCD 3000 camera (Jobin Yvon). Luminescence spectra were recorded by averaging the emission over at least 20 excitation pulses. Luminescence decay curves were recorded with a Hamamatsu R928 photomultiplier in combination with a digital oscilloscope (Tektronix TDS 3032B).

Acknowledgment. We thank Almut Barck for the XRD measurements, Sylvia Bartholdi-Nawrath and Andreas Kornowski for the TEM investigations, and Uwe Borchert for the light scattering measurements. This project was funded in part by the BMBF.

Supporting Information Available: Site-selective luminescence spectra of $LaPO_4:Eu^{3+}$ (1%) particles and luminescence decay curves of surface and bulk sites of $LaPO_4:Eu^{3+}$ (5%) nanoparticles. This material is available free of charge via the Internet at http://pubs.acs.org.

JA031826E